

Cathode Positioning System for Multiple Beam Electron Gun

V. Sinkevicius, D. Virzonis, L. Sumskiene, T. Jukna

Department of Electrical Engineering, KTU Panevezys Institute,

S. Daukanto str. 12, 35212 Panevezys, Lithuania; phone: +37045434247, e-mail: vytenis@elekta.lt, darius.virzonis@ktu.lt

Introduction

The requirements for the systems of the automated assembly of precise parts are becoming harder and harder in terms of rapidity, flexibility and accuracy. These qualities are achieved through the new technical solutions, such as multiple stage positioning. This is necessary when the assembled parts are to be quickly moved at the comparatively large distances (for example 10–100 mm) and positioned within comparatively narrow range of precision (for example, less than 1 μm). The flexibility problem arises, when the desired position of the part is partially uncertain, because it depends on the actual positions and geometric properties of another parts being assembled.

One stage positioning in such a case is difficult and expansive. From the one hand, this is because the ratio between the maximum distance at which the part is to be moved and the interval of the desired positioning is overcoming the order of 1000. From another – rapidity of the positioning is limited by the inertia and the friction forces of the actuator. In the two stage positioning design, the major part of the movement is performed by the one actuator and the precise part of the positioning – by another. This principle is well known in the context of positioning the magnetic disk heads [1]. The usual thing in industrial systems of automated assembly is the pneumatic actuator, responsible for the major part of the movement and the electromagnetic or piezoelectric actuator, responsible for the precision.

In the works of [2, 3] the capability of piezoelectric actuator to ensure the rapid positioning within the range of $\pm 0.1 \mu\text{m}$ is shown. Even the better results can be achieved on condition that maximum movement range is kept small. However, precise positioning in most cases is performed at comparatively low speed; therefore the impact of the friction forces is evident. Usually this undesired impact is of non-regular nature; therefore it can be hardly evaluated and eliminated. One of the solutions is the accelerometer, used for the active loop-back control of the actuating force [4]. Another solution is to reduce the still friction by applying vibrations to the friction surfaces [5]. The last is an attractive solution, because the source of vibrations can be applied to the static part of the actuator instead of additionally loading the moving part. The position sensor

in two stage positioning systems usually measures the position of the object itself and is not related to the kinematical parts [2, 3].

In our work we present the investigations of the dynamics and maximally allowable speed of the movement of the two stage drive, designated to position the cathodes in the multiple beam electron optics system (EOS). The properties of the position measurement system are explored too. In fact, the drive consists of one actuator for the major part of the movement (more than 150 mm) and three precision actuators, individually positioning each of three cathodes with the precision of $\pm 1 \mu\text{m}$. The possible desired positions are varying within the interval of 50 μm .

Peculiarities of the double stage drive

The task of the positioning system is to bring the cathodes in to the right position in respect of the modulator electrode. In previous work [6] an importance of the different individual positions of the cathodes was shown. As for as the distances between the electrodes of the assembled EOS have the deviations that affect significantly the cut-off voltages, the inter-electrode distances have to be measured and desired position of the cathodes calculated, basing on the results of the measurements. Moreover, the temperature deformations of the electrodes are to be evaluated. Due the absence of the adequate method of measuring the distance between the inner surfaces of the electrodes, the distance between the outer surfaces is measured and the inner distance is calculated evaluating thickness of the electrodes.

In the Fig. 1 the laps of the measurement of the inter-electrode distances and the operation of the cathode positioning drive is shown. The algorithm of the inter-electrode distances measurement incorporates also the cathodes positioning system operation. The EOS is manually placed on the base tubes, inside of which the measurement probes 3 are moved. During the first lap the probe 3 of the position sensor 2, under the action of the spring 1, is pressed forward to the accelerating electrode 4. The spring is acting with the average force of 60 G, assuring sufficient mechanical contact. The tip of the sensor probe 6 is getting through the hole 5 of the modulator. This base position is read and remembered individually for each cathode. During the second

positioning/measurement lap the piston 7 of the two-stage drive moves the cylindrical stick 8 until it rests to the surface of the modulator, simultaneously pushing the tip 6 and the probe 7 to the new position. A difference between these two positions is used to individually calculate the average distances between the modulator and the accelerating electrode. Now, when the inter-electrode distances of cold EOS are known, presumable distances at the working temperature are calculated [6]. From these results the desirable position of each cathode in respect of the corresponding part of the modulator is calculated.

During the third lap the cathode 9 is placed over the cylindrical stick 8 and moved by the piston 7 to the near proximity of the tip 6 of the measurement probe. Here the position of the piston is locked. Then the second stage of the drive 10, which is made of piezoelectric actuator, moves the cathode to the calculated position, at which cathode is to be laser welded. The position is tracked by the position sensor, being in contact with the cathode surface via the measurement probe and tip.

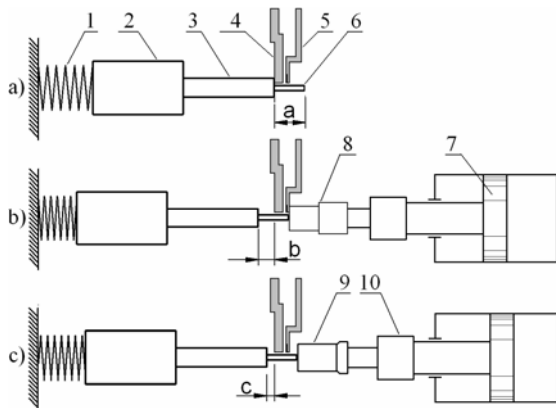


Fig. 1. Laps of the inter-electrode distance measurement and cathode positioning process: a – measurement of the accelerating electrode position, b – measurement of the modulator position, c – cathode positioning

When cathode is moved to the desired position, four stages of movement can be distinguished: movement of cathode to the near proximity of the tip, contact between the tip and the surface of the cathode, movement to the desired position and stop. Starting with the second of above mentioned stages, fragile surface of the oxide cathode is in mechanical contact with the probe tip. Especially hazardous is the moment when the moveless tip is hit by the surface of the moving cathode. Certain value of the pressure to the surface of the cathode has not to be overranged, keeping the surface of the cathode well. During the precision movement and stop, especially when the speed of the movement is near zero, the impact of the unstable friction forces (either still friction) becomes significant.

Dynamics of the drive during the hit

The maximum speed of the movement of the second stage of the drive is limited by the force, which originates from the interaction between the surfaces of the probe tip and the cathode. The force of the sensor spring, which

moves the probe, is complemented by the impact of the still friction during the hit. The surface of the cathode can be regarded as a resilient membrane, covered by the layer of powdery oxide. So the forces during the hit are to be adjusted so, that no footprints of the tip left on the oxide layer.

We performed series of dynamic experiments in order to determine possible impact of the hit between the cathode and the probe tip. The values of the probe movement were 10, 20, 60 and 80 mm/s. The actuator was stopped after the probe was hit by the cathode and displaced for 0.5 mm. After each experiment the surface of the cathode was visually examined by the microscopy. The footprints of the probe tip, corresponding to different speeds, are shown in the Fig. 2. The Fig. 3 illustrates the timed traces of the sensor readings at different cathode movement speeds.



Fig. 2. Footprints of the probe tip when the cathode is moved with different speeds

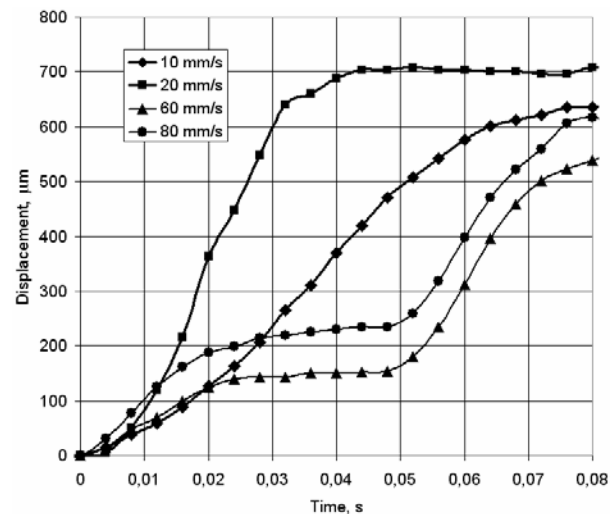


Fig. 3. Time traces of the probe movement when the cathode is moved with different speeds

We concluded that when the cathode is moved by the speed less than 10 mm/s, a hit between the cathode and the tip does not produce any noticeable harm to the oxide layer. When the speed of the cathode at the moment of the hit is greater than 30 mm/s, the forces, resisting to the movement of the probe, tend to overcome the fastness of the cathode surface. The oxide layer then is compressed and damaged, and the probe remains practically unmoved.

To be able to estimate the forces, acting to the surface of the cathode during the hit, we created simplified mathematical model of the cathode-probe system, structure of which is shown on the Fig. 4. As initial modelling conditions we regarded the moment, when the probe 2, actuated by the spring 1, rests by the step 3 to the

accelerating electrode 4. The tip of the sensor probe 6 is getting through the hole of modulator 5. Cathode, being moved by the constant speed v_k , touches the tip by the surface. The strain force, produced by the cathode surface, is modelled as a non-linear spring 7. We presumed that the surface of the probe strains like a membrane, which produces the fourth order dependency between the strain and strain induced force values.

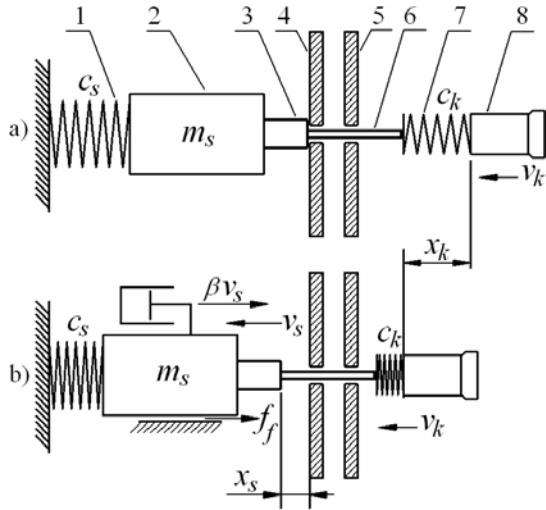


Fig. 4. Dynamic model: a – initial conditions, b – relationship between the moving parts

During the cathode positioning the spring of the sensor (1) is pressed, producing the force, increasing with the time. The dynamic behaviour of the system is described by the systems of equations (1) and (2), which evaluate the still friction, movement friction and the viscous friction.

$$\begin{cases} \frac{dv_s}{dt} = \frac{F(f_k, x_s, x_k, v_s) - \beta v_s}{m_s}, \\ \frac{df_k}{dt} = c_k (v_k(x_s) - v_s)^2 \text{sign}(v_k(x_s) - v_s), \\ \frac{dx_s}{dt} = v_s, \\ \frac{dx_k}{dt} = v_k(x_s), \end{cases} \quad (1)$$

where v_s – the speed of the measurement probe, x_s – displacement of the probe, $v_k(x_s)$ – function of the cathode speed, m_s – common mass of the probe and the moving part of the sensor, β – coefficient of viscous friction, c_k – equivalent tightness coefficient of cathode surface, x_k – cathode displacement, f_k – force, acting to the surface of the cathode.

The sum of the acting forces is described by the function (2). It also evaluates the different conditions of the movement. The first equation is applicable when the probe is unmoved. The purpose of the second equation is to evaluate the fact that the cathode surface is not connected to the probe tip, therefore the equivalent spring, representing the cathode surface, can not be stretched and

can not stop the backward movement of the probe. Hereby, when the condition $x_s > x_k$ is met, the probe is moved without the interaction with the surface of the cathode. The third equation is describing the movement, when the probe is pushed by the strained surface of the cathode

$$F(f_k, x_s, x_k, v_s) = \begin{cases} 0, & \text{if } [f_k - f_{tr0} - c_s(L_s + x_s)] \leq 0 \wedge x_s \leq 0, \\ -f_{tr} \text{sign}(v_s) - c_s(L_0 + x_s), & \text{if } x_s > 0 \wedge x_s > x_k, \\ f_k - f_{tr} \text{sign}(v_s) - c_s(L_0 + x_s), & \text{otherwise,} \end{cases} \quad (2)$$

where f_{tr0} – still friction force between the movement starts, c_s – coefficient of the tightness of the sensor spring, L_s – initial compression of the sensor spring, assuring the necessary force of resting the probe to the accelerating electrode, f_{tr} – friction force during the movement.

The speed of the cathode is described by the function (3). In general, this would be the variation of the speed of the second stage of the drive. Though, during the experimental investigation the maximum allowable speed of the cathode was determined. Therefore the cathode speed was described as follows:

$$v_k(x_s) = \begin{cases} v_{k0}, & \text{if } x_s \leq x_{max}, \\ 0, & \text{otherwise,} \end{cases} \quad (3)$$

where: v_{k0} – speed of the cathode, x_{max} – desired position of the cathode.

Modelling

Employing the previously described mathematical model we investigated the dynamics of the force of interaction between the tip and the cathode surface during the positioning process. The output of the model is presented at the Fig. 5. The actuator of the first positioning stage is stopped at the approximate position, just before the tips of the probes are being hit by the surfaces of the cathodes. The distance to be covered by the actuator of the second positioning stage until the hit will happen is generally unknown. So, we supposed the speed of the cathodes to be 10 mm/s and constant at the moment of the hit. The value of the still friction force was determined experimentally and used during modelling.

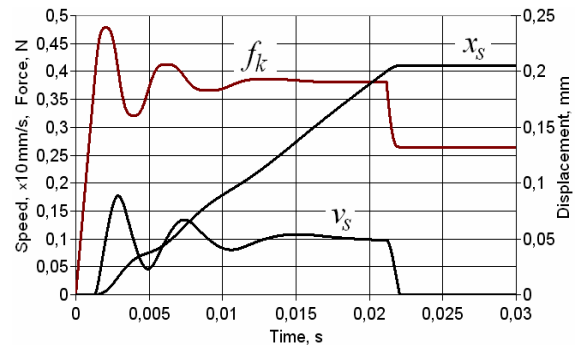


Fig. 5. Time traces of the force of interaction between the probe and the cathode, probe displacement and velocity ($\beta=3$)

All the rest of the parameters were taken from the real system. The actuator of the second stage is stopped at the position of $x_{max}=200 \mu\text{m}$. The lag of the probe movement in respect of the cathode movement is dependant on the tightness of the cathode surface and the value of the still friction force.

The influence of the value of the viscous friction coefficient β to the dynamics of the system, when the value of it varies from 2.5 to 32, is shown at the Fig. 6.

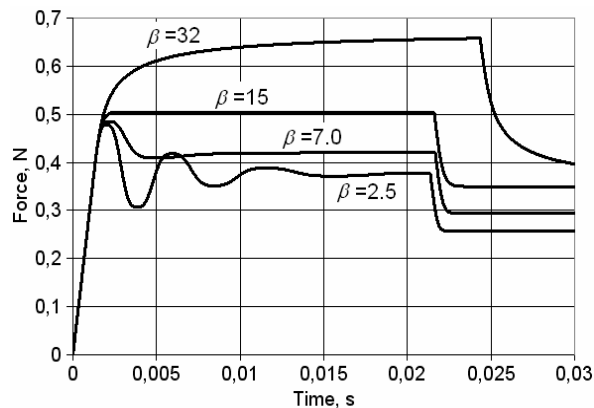


Fig. 6. Dynamics of the force of the interaction between the surface of the cathode and the probe tip with various values of the coefficient of the viscous friction β

Three qualitatively different ways of interaction were determined. When $\beta < 7$, the interaction is of the vibrating nature, which increases the uncertainty of the actual cathode position and increases the damage risk. When $10 < \beta < 18$, the interaction can be regarded as optimum, because the steady state of the system is reached rapidly. With the further increase of the β value the interaction force increases unacceptably.

Conclusions

Proposed dual stage positioning drive allows precise and rapid individual positioning of the multiple beam electron optical system cathodes.

Maximal allowable speed of the second stage actuator, securing the integrity of the cathode surface, was experimentally determined to be 10 mm/s.

The viscous friction force was determined to be the major factor influencing the value and dynamic behaviour of the cathode – probe interaction force.

References

1. Mori K. et al. A dual-stage magnetic disk drive actuator using a piezoelectric drive for a high track density // IEEE Trans. Magn.– 1991. – Vol. 27. – No. 6. – P. 5298–5300.
2. Yung-Tien Lu, Toshiro Higuchi. Precision Positioning Device Utilizing Impact Force of Combined Piezo-Pneumatic Actuator // IEEE/ASME Transactions on Mechatronics, 2001. – No. 4(6). – P. 467–473.
3. Katuhiro Nakaschima, Kazuki Takafuji, Yuuma Tamaru. Ultra Fine Positioning by Preload Change in Ball Screw Drive // Proceedings of the 1st International Conference on Positioning Technology, Japan; June 9–11, 2004. – P. 31–36.
4. Dunbar W. B., Callafon R. A., Kosmatka J. B. Coulomb and viscous friction fault detection with application to a pneumatic actuator // Advanced Intelligent Mechatronics, 2001.– Proceedings of IEEE/ASME International Conference, Como, Italy.– Vol.2. – P. 1239–1244.
5. Dupont P., Kasturi P., Stokes A. Semi-Active Control of Friction Dampers // Journal of Sound and Vibration. – 1997 – No. 2(202). – P. 203–218.
6. Jukna T., Sinkevicius V., Sumskiene L., Virzonis D. Research of the Electron Gun Cathode Tracking System // Electronics and Electrical Engineering. – Kaunas: Technologija, 2005. – No. 5(61). – P. 48–51.

Submitted for publication 2006 03 10

V. Sinkevicius, D. Virzonis, L. Sumskiene, T. Jukna. Cathode Positioning System for Multiple Beam Electron Gun // Electronics and Electrical Engineering. – Kaunas: Technologija, 2006 – No. 5(69). – P. 21–24.

The results of the investigations of the dual-stage cathode positioning system with more than 150 mm motion range and $\pm 1 \mu\text{m}$ positioning accuracy are presented. The maximum allowable speed of the second stage actuator, securing the integrity of the cathode surface, of 10 mm/s was determined experimentally. The dynamic model of the cathode-probe system allowed to explore the dynamics of the interaction force and the dependencies of their character on the viscous friction. Ill. 6, bibl. 6 (in English; summaries in English, Russian and Lithuanian).

V. Синкявичюс, Д. Вирзонис, Л. Шумскене, Т. Юкна. Система позиционирования катодов многолучевой электронно-оптической системы // Электроника и электротехника. – Каунас: Технология, 2006 – № 5(69). – С. 21–24.

Представлены результаты исследований двухступеневой системы позиционирования катодов с возможностью передвижения до 150 мм и точностью позиционирования $\pm 1 \mu\text{m}$. Экспериментально установлено, что максимальная скорость передвижения вторичного привода при условии невредимости поверхности катода составляет 10 мм/с. Динамическая модель системы катод-измерительный штырь позволила исследовать динамику силы взаимодействия элементов системы и зависимость ее характера от вязкого трения. Ил. 6, библи. 6 (на английском языке; рефераты на английском, русском и литовском яз.).

V. Sinkevičius, D. Virzonis, L. Šumskienė, T. Jukna. Elektronų prožektoriaus katodų pozicionavimo sistema // Elektronika ir elektrotechnika. – Kaunas: Technologija, 2006 – Nr. 5(69). – P. 21–24.

Pateikti tiesiaieigės dvipakopės katodų pozicionavimo pavaros, turinčios didesnę nei 150 mm eigą ir $\pm 1 \mu\text{m}$ pozicionavimo tikslumą, tyrimų rezultatai. Eksperimentiškai nustatyta, kad, nesukeliant katodo paviršiaus pažeidimo, maksimalus katodo judesio greitis jo padėties tikslaus derinimo metu gali būti iki 10 mm/s. Eksperimentiniai ir realios sistemos duomenimis pagrįstas katodo ir liestuko sistemos dinaminis modelis leido iširti jėgų, veikiančių paviršių jo pozicionavimo metu, dinamiką ir jos pobūdžio priklausomybes nuo klampiosios trinties. Il. 6, bibl. 6 (anglų kalba; santraukos anglų, rusų ir lietuvių k.).